Available online at www.sciencedirect.com
ScienceDirect
Carbon 45 (2007) 821–827
CARBON
www.elsevier.com/locate/carbon

Reflection and absorption contributions to the electromagnetic interference shielding of single-walled carbon nanotube/polyurethane composites

Zunfeng Liu, Gang Bai, Yi Huang, Yanfeng Ma, Feng Du, Feifei Li, Tianying Guo, Yongsheng Chen *

Key Laboratory for Functional Polymer Materials & Center for Nanoscale Science and Technology, Institute of Polymer Chemistry, Nankai University, Tianjin 300071, China

Received 1 August 2006; accepted 17 November 2006
Available online 19 January 2007

Abstract

The electromagnetic interference (EMI) shielding of well dispersed single-walled carbon nanotube (SWCNT)/polyurethane composites was studied and the results show that they can be used as effective and lightweight shielding materials. The EMI shielding of the composite shows a reflection-dominant mechanism, while a shift from reflection to absorption was observed with increased SWCNT loading and frequency. This is explained using EMI shielding theory and the intrinsic properties of the components.

1. Introduction

As commercial, military, and scientific electronic devices and communication instruments are used more and more widely, electromagnetic interference (EMI) shielding of radio frequency radiation continues to be a more serious concern in this modern society. Light weight EMI shielding is needed to protect the workspace and environment from radiation coming from computers and telecommunication equipment as well as for protection for sensitive circuits [1]. Compared to conventional metal-based EMI shielding materials, electrically conducting polymer composites have gained popularity recently because of their light weight, resistance to corrosion, flexibility and processing advantages [2–9]. The EMI shielding efficiency (SE) of a composite material depends on many factors, including the filler's intrinsic conductivity, dielectric constant, and aspect ratio [7,9]. The high conductivity, small diameter, high aspect ratio, and super mechanical strength and so on of carbon nanotubes (CNTs) make them an excellent option to create conductive composites for high-performance EMI shielding materials at low filling concentration. Recently, multi-walled carbon nanotubes (MWCNTs) have been studied with various polymer matrix, including polystyrene (PS) [1], epoxy [10], poly(methyl methacrylate) (PMMA) [11], polyaniline (PANI) [1], polypyrrole (PPY) [1], PU [10,12,13], etc., for the possible applications as effective and light weight EMI shielding materials and the EMI shielding has been attributed mainly due to the reflection contribution [10,14,15]. When Fe is hybridized with CNT/polymer composites, it is observed that the main contribution to total EMI SE is absorption rather than reflection [16,17]. Also the influences of wall defects [10], aspect ratio [10], and alignment [18] of CNTs on the EMI shielding have been investigated. But the composite materials with single-walled carbon nanotubes (SWCNTs) have been largely unexplored for this area so far [10,12]. Very recently we reported the first EMI shielding study of the composite materials of SWCNTs with epoxy as matrix in the frequency range of 10 MHz–1.5 GHz [10]. But owing to many different, and in many cases superior, properties compared with MWCNTs, SWCNTs warrant more studies for light and effective EMI shielding materials.

* Corresponding author. Tel.: +86 22 2350 0693; fax: +86 22 2349 9992.
E-mail address: yschen99@nankai.edu.cn (Y. Chen).

0008-6223/$ - see front matter © 2006 Elsevier Ltd. All rights reserved.
doi:10.1016/j.carbon.2006.11.020

Polyurethane (PU) elastomers are widely used high-performance materials with many unique properties, including good elasticity, high impact strength and elongation, resistance to low temperature, and excellent bio-compatibility [19,20]. And these properties have made them widely used in many civil and military industries [21]. In this paper we prepared well dispersed PU/SWCNT composites using a simple physical blending method. An EMI SE up to 17 dB at the band range of 8.2–12.4 GHz (so called X band) was obtained for PU/SWCNT composites with 20 wt% SWCNT loading. The composites show a percolation threshold as low as ~0.2 wt%. The investigation in the shielding mechanism shows a reflecting-dominant mechanism, whereas a contribution shift behavior toward to absorption was observed with increased SWCNT loading and frequency. Using EMI shielding theory, this trend is explained with the intrinsic properties of the components. At high SWCNT loadings and we found the intrinsic properties favored the absorbing ability rather than the reflecting one.

2. Experimental

2.1. Materials and measurements

SWCNTs were prepared in our laboratory using a modified arcing method [22]. Using AFM [23], we found the bundles for the raw SWCNTs (AP SWCNTs) had an average diameter = 5.95 nm, average length = 1430 nm. The AP SWCNTs have specific surface area of 1500 m^2/g and contain about 50 wt% SWCNTs. *N*,*N*-dimethyl formamide (DMF, AR) was used as purchased. Polyurethanes were supplied by Tianjin Polyurethane Co. ($Mn = 20{,}000$, hardness = 85, density = 1.34, synthesized from Diphenyl methane 4,4-diisocyanate (MDI), 1,4-butadiol, and polyethylene glycol adipate ($Mn = 1000$)).

The dc electrical conductivity of the SWCNT-epoxy composites was determined using the standard four-point contact method on rectangular sample slabs in order to eliminate contact-resistance effects at room temperature. Data were collected with a Keithley SCS 4200. The EMI shielding effectiveness and complex (relative) permittivity data of SWCNT/PU composites were measured with the slabs of dimension of 22.86 mm × 10.16 mm × 2 mm to fit waveguide sample holder using a HP vector network analyzer (HP E8363B) in 8.2-12.4 GHz (X band). And total 201 data points were taken within this frequency range for each sample. The PU/SWCNT samples were freeze-fractured in liquid nitrogen and gold coated for imaging on a Hitachi S-3500 N scanning electron microscope (SEM).

2.2. Preparation of the PU/SWCNT composites and their films

We used the conventional solution process to prepare the composites and their films. As an example, the following describes the process to prepare the composite with 5 wt% SWCNT loading. SWCNTs (2.15 g) were added into DMF (1500 mL), stirred for 2 h, and then the mixture was sonicated for 2 h using a high power sonic bath (300 W, modeled KQ-300DB) to disperse SWCNTs in DMF. Then PU (43 g) dissolved in 300 mL of DMF was added to above SWCNT suspension and the formed mixture was then stirred mechanically for 2 h. The mixture was further sonicated for 2 h using the above sonic bath. Note that more DMF (to keep SWCNT concentration to be ~1.5 mg/mL) was used for higher SWCNT loading composites. After the mixture was again stirred mechanically for 2 h, it was then cast in a large mold to let solvent to evaporate at ~140 °C. Then the PU/SWCNT films were pealed off from the mold and vacuum dried at 80 °C for 48 h. After a hot pressure process at 150 °C and 15 MPa, a flat film of PU/SWCNT composite with 5 wt% SWCNT loading was obtained. The sample was then cut to slabs with desired sizes and then the surfaces of the slabs were polished if necessary. Other composites with different loadings were prepared similarly. As a control, pure PU films and slabs were prepared using the same process.

3. Results and discussion

3.1. Theoretical background

For a transverse electromagnetic wave propagating into a sample with negligible magnetic interaction, the total shielding efficiency (SE_T) of the sample is expressed as Eq. (1) [7,24,25]:

$$SE_T = 10\log(P_{in}/P_{out}) = SE_A + SE_R + SE_I \quad (1)$$

where P_{in} and P_{out} are the power incident on and transmitted through a shielding material. The SE_T is expressed in decibels (dB). The SE_A and SE_R are the absorption and reflection shielding efficiencies, respectively. The third term (SE_I) is a positive or negative correction term induced by the reflecting waves inside the shielding barrier (multi-reflections), which is negligible when $SE_A \geqslant 15$ dB [24,25]. The terms in Eq. (1) can be described as

$$SE_A = 8.68\alpha l \quad (2)$$

$$SE_R = 20\log\frac{|1+n|^2}{4|n|} \quad (3)$$

$$SE_I = 20\log\left|1-\frac{1-n^2}{1+n^2}\exp(-2\gamma l)\right| \quad (4)$$

where the parameters α, n, and γ are defined as following equations, l is the thickness of the shielding barrier.

$$\alpha = (2\pi/\lambda_0)\sqrt{\frac{\varepsilon_r(\sqrt{1+\tan^2\delta}\mp 1)}{2}} \quad (5)$$

$$n = \sqrt{\frac{\varepsilon_r(\sqrt{1+\tan^2\delta}\pm 1)}{2}} + i\sqrt{\frac{\varepsilon_r(\sqrt{1+\tan^2\delta}\mp 1)}{2}} \quad (6)$$

$$\gamma = (2\pi/\lambda_0)\sqrt{\frac{\varepsilon_r(\sqrt{1+\tan^2\delta}\mp 1)}{2}} + i(2\pi/\lambda_0)\sqrt{\frac{\varepsilon_r(\sqrt{1+\tan^2\delta}\pm 1)}{2}} \quad (7)$$

where λ_0 is the wave length, ε_r the real part of complex relative permittivity, the $\pm$ and $\mp$ signs are applied for positive and negative ε_r, respectively.[25] The loss tangent tan $\delta = \varepsilon_i/\varepsilon_r = \sigma\varepsilon_0\varepsilon_r$, where ε_i is the imaginary part of the relative permittivity; $\omega = 2\pi F$, where F is the frequency; ε_0 is the dielectric constant in free space and σ the conductivity. Here we use the alternative conductivity (σ_{ac}) to express the conducting ability of the alternative electromagnetic wave in the composites: $\sigma_{ac} = \omega\varepsilon_0\varepsilon_r$. The estimation of the SE in this study is in the far-field limit [25], which assumes that the distance from the source to the shielding barrier is long enough and not to apply near-shielding effects. From Eqs. (1)–(7), SE_T is tuned by α, n, and l. The intrinsic parameters for the SE_T are α and n, which are determined by ε_r and σ_{ac}. From these equations, one can expect high shielding efficiency for materials with higher ε_r and σ_{ac}. The thickness of the material l is an extrinsic parameter which can be used to control SE_A and SE_I. The imaginary part of the complex permittivity ε_l, also called loss factor, indicates the ability of the materials to absorb radio wave. The term tan δ, also called loss tangent, indicates the ability of a material to convert stored energy to heat. Thus, large values of loss factor and loss tangent would indicate a better radio absorbing material [26].

The material with tan $\delta \gg 1$ exhibits as a good conductor and the material with tan $\delta \ll 1$ exhibits as a weak conductor [27]. In case of tan $\delta \gg 1$, α can be approximated as $\alpha \approx (\omega\mu\sigma/2)^{1/2}$ and $n \approx (1 + i)(\sigma/2\omega\varepsilon)^{1/2}$, where μ is the permeability. This indicates that for the highly conducting materials, the EMI shielding (including absorption and reflection) shall be decided mainly by σ, not ε_r. In the case of tan $\delta \ll 1$, $\alpha \approx (\sigma/2)(\mu/\varepsilon_0\varepsilon_r)^{1/2}$, indicating that the electromagnetic energy dissipation can also occurred in the weak conductors where permeability plays a more important role. In the present study however, tan $\delta \approx 1$ (see below), so the above approximated formulas can not be used, and both σ_{ac} and ε_r must be considered when estimating the EMI shielding efficiency.

3.2. DC conductivity of the PU/SWCNT composites

As seen from the EMI theory above, the EMI performance of composites is highly coupled with the filler's intrinsic conductivity, dielectric constant, and aspect ratio[7,9]. Fig. 1 shows the dc conductivity (σ_{DC}) of PU/SWCNT composites as a function of SWCNT mass fraction (p). As can be seen, the conductivity of the PU/SWCNT composites exhibits a dramatic increase at low loadings, indicating the formation of percolating network. For example, below 0.25 wt%, the conductivity of SWCNT composites displays a dramatic increase of 6 orders of magnitude and the conductivity reaches 2.2×10^{-4} S/cm at 20 wt% SWCNT loading. This value is 10 orders of magnitude higher than that of the pure PU matrix (i.e., 1.2×10^{-14} S/cm).

Thus far, studies on the conductivity of SWCNT–polymer composites have been reported low thresholds at various volume fractions with different fabrication methods and different SWCNT aspect ratio [8,28]. For real applications, it is critical to have low filling threshold, since lower filling fractions imply smaller perturbations of bulk physical properties as well as lower cost. It is well known that the conductivity of a conductor–insulator composite follows the critical phenomena around the percolation threshold (Eq. (8)) [29]:

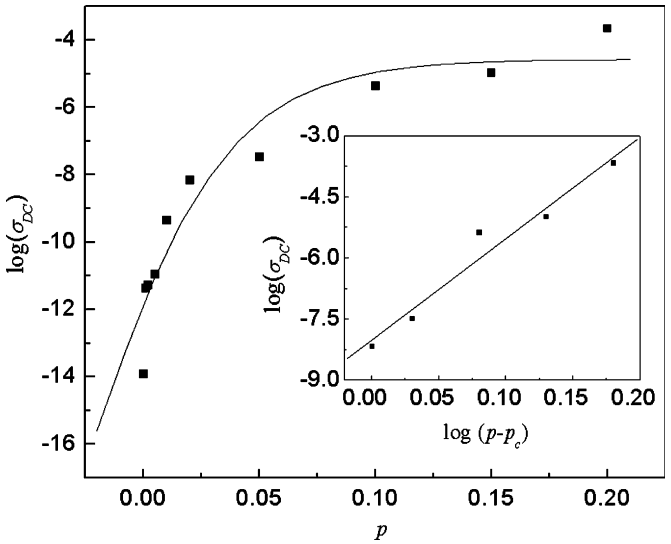

Fig. 1. DC conductivity (σ_{DC}) *vs* weight percentage (p) of PU/SWCNT composites at room temperature. The inset shows the log–log plot of σ_{DC} to $(p - p_c)$.

$$\sigma_{DC} \propto (v - v_c)^{\beta} \tag{8}$$

where σ_{DC} is the composite conductivity, v is the SWCNT volume fraction, v_c is the percolation threshold and β is the critical exponent. Because the densities of the polymer and SWCNTs are similar, we assume that the mass fraction, p, and the volume faction, v, of the SWCNTs in the polymer are almost the same. As shown in the inset to Fig. 1 for the log (σ_{DC}) vs log ($p - p_c$) plot, a least-squares analysis of the fits using Eq. (1), shows that the threshold volume p_c for the composites was strongly bounded by the regions between the highest insulating and lowest conducting points and the PU/SWCNT composite conductivity agrees very well with the percolation behavior predicted by Eq. (8).

The best fit of the conductivity data to the log-log plot of the power laws gave $p_c \approx 0.2\%$, and $\beta = 3.74$, according to Eq. (8), as shown in the inset in Fig. 1. While computer models of conductivity percolation give a critical exponent value of 2 for a 3-d rigid rod network, various values from 1.3 to 5.3 have been reported for different CNT-polymer composites. These included SWCNT composites with critical exponent values of 1.5 for polyimide [30], 1.3 and 2.68 for epoxy [10,28], and 2–3 for different SWCNT materials with epoxy [8]. Similarly, various values from 2.15 to 5.31 for MWCNT composites have been reported [17]. A percolation threshold of ~16% has been predicted in two-phase random composites when the conducting micro scaled fill-

ers with sphere shape are used. However, the percolation threshold $p_c \approx 0.2$ wt% in this work is ~2 orders smaller than the theoretical result and also comparable to other SWCNT composite materials [8,28,31]. This low threshold value can be attributed to the large one dimensional aspect ratio and well dispersion of SWCNTs in the composites. The well dispersion was also confirmed with the SEM image in Fig. 2 for the 20 wt% loading of SWCNTs. The SEM image clearly shows that the SWCNTs were distributed rather homogeneously. Note electrostatic dissipation applications typically require a conductivity of 10^{-5} S/cm and thus with only addition of 5 wt% SWCNTs, these PU/SWCNT composites should be able to be used for many electrostatic dissipation applications too.

3.3. Complex relative permittivity vs SWCNT loadings and frequencies

Recent studies have shown that SWCNT/polymer composites posses high real permittivity (polarization, ε_r) as well as imaginary permittivity (adsorption or electric loss factor, ε_i) in the 0.5–2 GHz [10] and 500 MHz–5.5 GHz ranges [32], indicating that SWCNT/polymer composites could be used as light weight and effective electromagnetic shielding materials. We thus measured the complex permittivity of SWCNT/PU composites in the frequency range of 8.2–12.4 GHz (X band). Fig. 3 shows the complex relative permittivity spectra of the composites containing 0%–20 wt% SWCNTs. As can be seen, the real (ε_r) and imaginary (ε_i) permittivity increase dramatically as the concentration of SWCNTs increases from 5 to 20 wt%. The highest values of the real and imaginary permittivity parts for the composite with 20 wt% SWCNT loading reach 38 and 26, respectively. Overall the real and imaginary parts of permittivity for this PU/SWCNT composites with 20 wt% SWCNTs range from 32 to 38 and 24 to 26 in the frequency of 8.2–12.4 GHz. Furthermore, at low loadings, both the real and imaginary parts of permittivity are almost independent to the frequencies in the range we measured with the same loading. But at higher (e.g. 20 wt%) loading, the values of the real part of the permittivity intend to decrease with increasing of frequency, while the imaginary values still keep little change. The absolute values of the measured permittivity are of the same order of magnitude as those reported by Grimes et al. for SWCNT/polymer composites in the 0.5–5.5 GHz range [32]. These trends are important to understand the EMI mechanism discussed below. A peak between 8.5 and 9.5 GHz was found for the composites (10, 15, and 20 wt%) and it becomes stronger with higher SWCNT loadings. This result implies the existence of a resonance behavior, which is expected when the composite is highly conductive and skin effect becomes significant [16]. Che et al. [16] reported that the frequency at which the peak occurs is determined by the aspect ratio of the nano-scaled

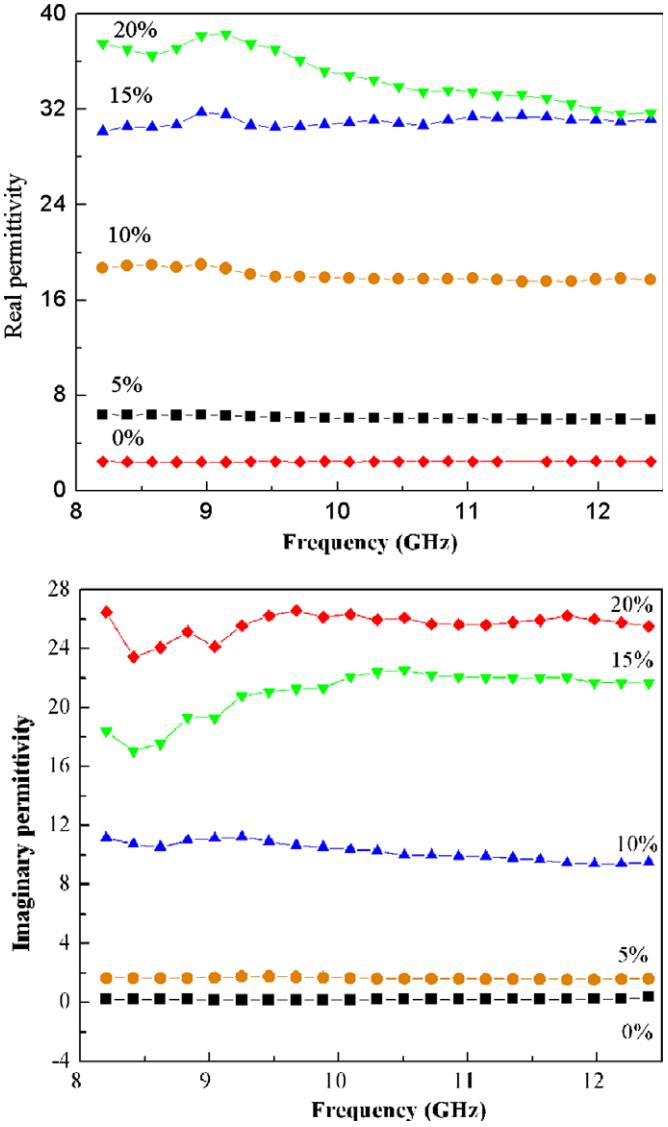

Fig. 3. Real (ε_r) and imaginary (ε_i) parts of the relative permittivity in the frequency range of 8.2–12.4 GHz.

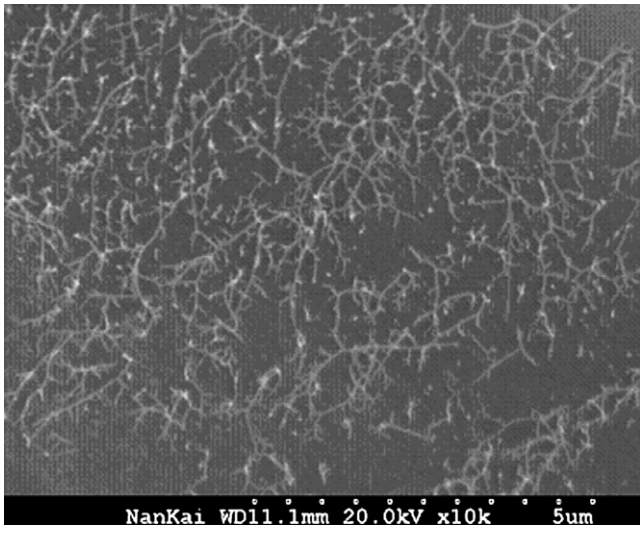

Fig. 2. A typical SEM image of PU/SWCNT composite containing 20 wt% SWCNTs after freeze-fractured in liquid nitrogen and gold coated.

fillers and they found that the Fe-encapsulated carbon nano-cages have a peak at about 5 GHz and the Fe-encapsulated MWCNTs have a peak at about 7 GHz. In this paper, the composites have a resonance peak at about 9 GHz. This is probably because a high aspect ratio of SWCNTs compared to that of MWCNTs.

3.4. EMI shielding effectiveness of the PU/SWCNT composites

Fig. 4 shows the EMI shielding effectiveness over the frequency range of 8.2–12.4 GHz for PU/SWCNT composites with various SWCNT loadings. As expected from the above data about conductivity and permittivity, the EMI shielding effectiveness increases with increasing content of SWCNTs in the composite and the contribution to the EMI shielding should come from the addition of SWCNTs. It is also observed that the shielding effectiveness of the composites almost keeps unchanged except for a slight decrease with increasing the frequency for the same loading. The shielding effectiveness of the composites containing 20 wt% SWCNTs is measured to be 16–17 dB over the frequency range of 8.2–12.4 GHz.

Fig. 5 shows the tan δ values of the composites, from which it can be seen that the tan δ values of the composites are in the range of 0.25–0.8, very close to 1, indicating that the composites in this work do not act as good nor weak conductors [27]. Therefore the intrinsic parameters ε_r and σ_{ac} must be considered to evaluate the EMI SE. The EMI SE was thus plotted versus ε_r and σ_{ac}, respectively at 8.2 GHz as an example in Fig. 6. The data in Fig. 6 fall on smooth curves, and similar dependence of EMI SE on σ_{ac} and ε_r was obtained. From the fitted curve in Fig. 6a, we can see a dramatic increase in shielding effectiveness with the initial variation of σ_{ac}, and then EMI SE increases slowly with the continuous increase in σ_{ac}. A similar trend

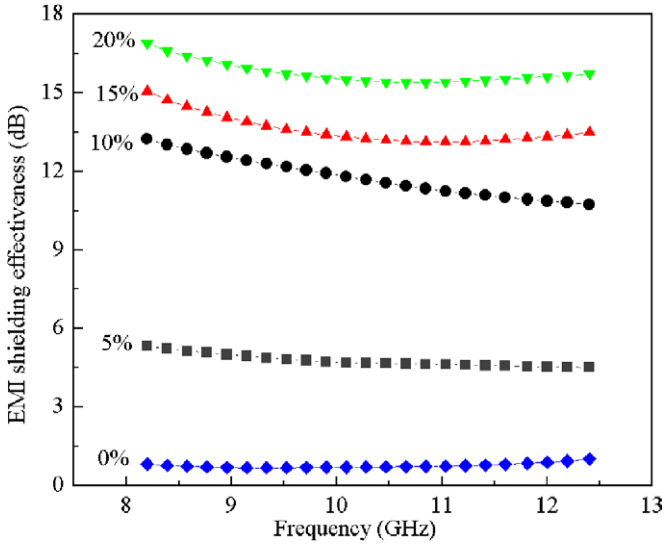

Fig. 4. EMI shielding effectiveness for PU/SWCNT composites in the frequency range of 8.2–12.4 GHz.

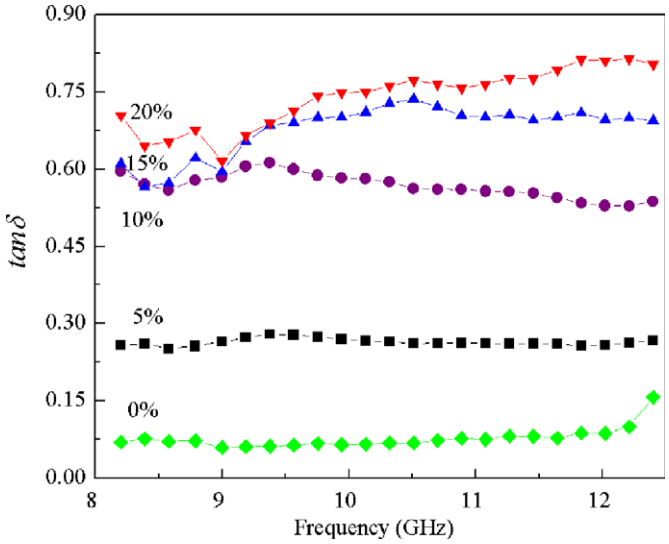

Fig. 5. The tan δ values of PU/SWCNT composites in the frequency range from 8.2 to 12.4 GHz.

was observed for the plotting of EMI versus ε_r. Recall that both σ_{ac} and ε_r increase with SWCNT loadings in Figs. 1 and 3. The above results indicate that EMI shielding effectiveness increases much faster at low SWCNT loadings, which becomes slower with higher SWCNT loadings.

3.5. Contribution shift from reflection to absorption at higher SWCNT loading and frequency

As discussed in Section 3.1, the EMI SE has three contributions: reflectivity (R), Absorptivity (A) and the multi-reflecting correction of waves inside the shielding barrier. For a very approximate analysis, the multi-reflecting part could be neglected, particularly for the cases when total $SE_A > 15$ dB. Thus we could use the equation of $100\% = A + T + R$ to get all the values of A from the experimental results of T and R to evaluate each contribution for the total shielding. The results are summarized in Fig. 7.

From Fig. 7, it can be seen that the major contribution for EMI SE still comes from the reflection; which is consistent with the literatures [14,15] for CNT composites. At low loadings, both A and R increases with increasing loading. More interestingly, we can see a general trend at high loadings (e.g. >10 wt% loadings) that the absorption contribution for EMI shielding increases while the reflection contribution decreases with the increase in the SWCNT loading at the same frequency. For example, in the case of the results at 12.4 GHz, the reflectivity of the composite with a $p = 5$ wt% is as high as 46.4%, and the absorptivity 18.3%. As the p increases to 10 wt%, the reflectivity increases to 69.8% and the absorptivity increases slightly to 21.7%. As the p continues to increase to 15 wt%, a contribution shift behavior is observed: the reflectivity decreases from 69.8% to 52.8% and the absorptivity increases to 42.7%, almost doubles the one at 10 wt% SWCNTs' loading (21.7%). As the p continues to increases

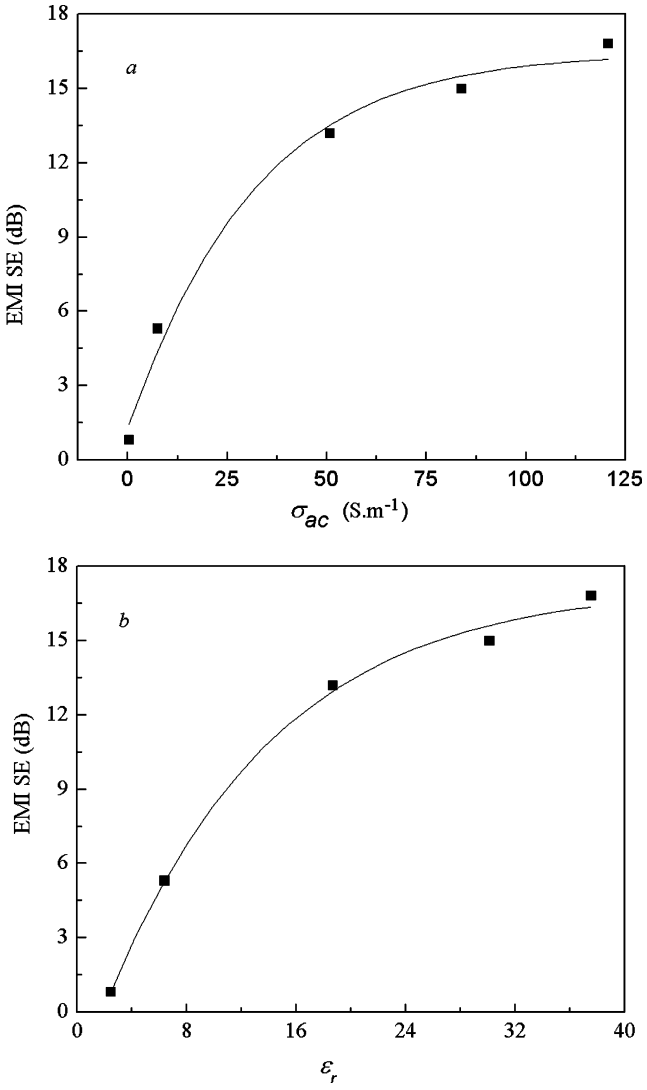

Fig. 6. The EMI SE at 8.2 GHz as a function of σ_{ac} (a) and ε_r (b) for the PU/SWCNT composites.

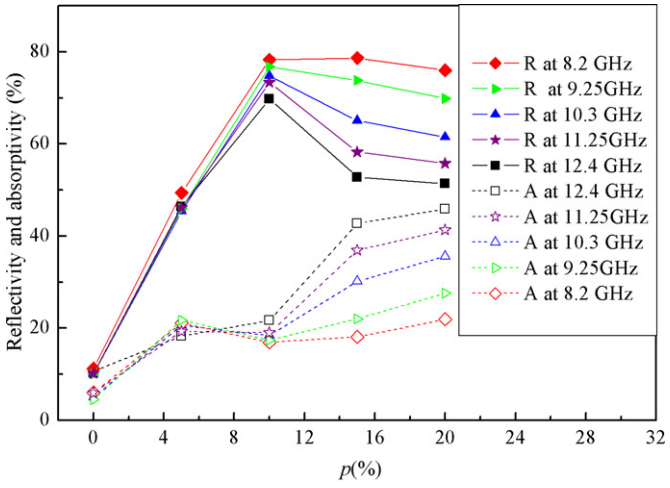

Fig. 7. Reflectivity (R) and absorptivity (A) vs SWCNT loadings at different frequencies.

to 20 wt%, the reflectivity continues to decreases to 51.4% and the absorptivity increases to 45.9%. Furthermore, the higher the frequency, the more evident the trend is.

Such a contribution shift behavior relates closely to the inner properties of the composite. As we know that the loss tangent tan δ indicates the ability of a material to convert stored energy into heat, i.e., tan δ provides an indication for how well the material can be penetrated by an electrical field and how well it dissipates electromagnetic energy as heat. It can be seen from Fig. 5 that tan δ increases with the increase in SWCNT loadings. Tan δ is almost zero for the sample without SWCNTs, indicating pure PU can hardly attenuate/absorb the radio wave. As SWCNT loading increases to 5 wt% and 10 wt%, tan δ increases to ~0.25 and 0.55, respectively. Thus A values increase as observed in Fig. 7. This is also evident from Eqs. (2)–(6). From Eqs. (2)–(6), we can see at higher frequency, with increasing tan δ, SE_A shall increase faster than SE_T.

A similar trend was found as the increase of frequency with the same SWCNT loading from Fig. 7, i.e., the reflectivity decreases and absorptivity increases for the same loading of SWCNTs . For example, for the case of $p = 20$ wt%, the reflectivity decreases from 76.0% to 61.5% and then to 51.4% as the frequency increases from 8.2 to 10.3 and then to 12.4 GHz. Such a contribution shift behavior is more evident for the samples with a higher loading.

Again this trend could be understood from Figs. 3 and 5 and Eq. (2)–(6). At the same loading, we can see the values of tan δ increases as frequency increases but the ε_r keeps almost unchanged at lower loading and slightly decreases with higher loadings (see Fig. 3). Recall the tan δ indicates the material capability to absorb radio wave energy; the above trend thus would become expected. This can also be evident from Eq. (2)–(6), as SE_A would increase relatively faster than SE_R when ε_r keeps almost unchanged with increasing tan δ for the same loading of SWCNTs.

From Fig. 6 it can be seen that at the initial stage, EMI SE increases much faster with increase of σ_{ac} and ε_r and from Fig. 7 we can see a greater increase in R and a smaller increase in A at the same stage. This indicates that at low SWCNT loadings, σ_{ac} and ε_r affect more R than A with the increasing SWCNT loading. Also from Fig. 6 in the region with high values of σ_{ac} and ε_r, EMI SE increases slower and from Fig. 7 we can see a decrease in R and an increase in A. These results thus indicates that at high SWCNT loading, σ_{ac} and ε_r contributes more to A than to R with increasing SWCNT loading.

4. Conclusion

In this paper, PU/SWCNT composites with well-dispersed SWCNTs were prepared using a simple physical mixing method and an EMI shielding effectiveness of ~17 dB was achieved at the SWCNT loading of 20 wt%. Together with PU excellent properties and wide applications, the EMI shielding properties endowed by SWCNT

as a filler shall make these composites one of the ideal candidates for EMI application. The EMI shielding of the composites show a reflecting-dominated mechanism, whereas with the increase in SWCNT loading and the frequency, a contribution shift from reflection to absorption was observed at higher loadings. By analyzing the transmission behavior of the electromagnetic wave and the intrinsic properties of the composites, we attribute this phenomenon to the increase of the tan δ due to the increase of the imaginary part of the dielectric constant of the composite materials. Our observations call for a better understanding for the EMI shielding mechanism to optimize the design of EMI shielding materials using SWCNTs. Future work will concentrate on studies for this energy transition behavior and the application of this property in electromagnetic wave absorption.

Acknowledgements

We gratefully acknowledge the financial support from MOST (#2003AA302640 and 2006CB0N0700), MOE (#20040055020) and the NSF Tianjin (#043803711) of China.

References

[1] Wang Y, Jing X. Intrinsically conducting polymers for electromagnetic interference sheilding. Polym. Adv. Technol. 2005;16(4):344–51.
[2] Yang YL, Gupta MC, Dudley KL, Lawrence RW. Conductive carbon nanofiber-polymer foam structures. Adv. Mater. 2005;17(16): 1999–2003.
[3] Xiang CS, Pan YB, Liu XJ, Sun XW, Shi XM, Guo JK. Microwave attenuation of multiwalled carbon nanotube-fused silica composites. Appl. Phys. Lett. 2005;87(12):1231031–3.
[4] Joo J, Epstein AJ. Electromagnetic-radiation shielding by intrinsically conducting polymers. Appl. Phys. Lett. 1994;65(18):2278–80.
[5] Luo X, Chung DDL. Electromagnetic interference shielding reaching 130 dB using flexible graphite. Carbon 1996;34(10):1293–4.
[6] Luo XC, Chung DDL. Electromagnetic interference shielding using continuous carbon-fiber carbon-matrix and polymer-matrix composites. Composites Part B 1999;30(3):227–31.
[7] Joo J, Lee CY. High frequency electromagnetic interference shielding response of mixtures and multilayer films based on conducting polymers. J. Appl. Phys. 2000;88(1):513–8.
[8] Bryning MB, Islam MF, Kikkawa JM, Yodh AG. Very low conductivity threshold in bulk isotropic single-walled carbon nanotube-epoxy composites. Adv. Mater. 2005;17(9):1186–91.
[9] Chung DDL. Electromagnetic interference shielding effectiveness of carbon materials. Carbon 2001;39(2):279–85.
[10] Li N, Huang Y, Du F, He X, Lin X, Gao H, et al. Electromagnetic interference (EMI) shielding of single-walled carbon nanotube epoxy composites. Nano Lett. 2006;6(6):1141–5.
[11] Kim HM, Kim K, Lee SJ, Joo J, Yoon HS, Cho SJ, et al. Charge transport properties of composites of multiwalled carbon nanotube with metal catalyst and polymer: application to electromagnetic interference shielding. Curr. Appl. Phys. 2004;4(6):577–80.
[12] Ma CCM, Huang YL, Kuan HC, Chiu YS. Preparation and electromagnetic interference shielding characteristics of novel carbon-nanotube/siloxane/poly-(urea urethane) nanocomposites. J. Polym. Sci., Part B: Polym. Phys. 2005;43(4):345–58.
[13] Wu HL, Ma CCM, Yang YT, Kuan HC, Yang CC, Chiang CL. Morphology, electrical resistance, electromagnetic interference shielding and mechanical properties of functionalized MWNT and poly(urea urethane) nanocomposites. J. Polym. Sci., Part B: Polym. Phys. 2006;44(7):1096–105.
[14] Yang YL, Gupta MC. Novel carbon nanotube-polystyrene foam composites for electromagnetic interference shielding. Nano Lett. 2005;5(11):2131–4.
[15] Yang YL, Gupta MC, Dudley KL, Lawrence RW. A comparative study of EMI shielding properties of carbon nanofiber and multiwalled carbon nanotube filled polymer composites. J. Nanosci. Nanotechnol. 2005;5(6):927–31.
[16] Che RC, Peng LM, Duan XF, Chen Q, Liang XL. Microwave Absorption Enhancement and Complex Permittivity and Permeability of Fe Encapsulated within Carbon Nanotubes. Adv. Mater. 2004; 15(5):401–5.
[17] Kim HM, Kim K, Lee CY, Joo J, Cho SJ, Yoon HS, et al. Electrical conductivity and electromagnetic interference shielding of multiwalled carbon nanotube composites containing Fe catalyst. Appl. Phys. Lett. 2004;84(4):589–91.
[18] Cheng HZ, Jou WS, Lin PT, Huang CC, Chen EC. A novel CNTS/polymer/PE composite with high electromagnetic shielding. Annu. Tech. Conf. Antec. Conf. Proc. 2004;2:1662–7.
[19] Li YJ, Hanada T, Nakaya T. Surface modification of segmented polyurethanes by grafting methacrylates and phosphatidylcholine polar headgroups to improve hemocompatibility. Chem. Mater. 2006; 11(3):763–70.
[20] Shirasaka H, Inoue S, Asai K, Okamoto H. Polyurethane urea elastomer having monodisperse poly(oxytetramethylene) as a soft segment with a uniform hard segment. Macromolecules 2000; 33(7):2776–8.
[21] Randall D, Lee S. The Polyurethanes Book. New York: John Wiley & Sons; 2002. 5-30.
[22] Lv X, Du F, Ma Y, Wu Q, Chen Y. Synthesis of high quality single-walled carbon nanotubes at large scale by electric arc using metal compounds. Carbon 2005;43(9):2020–2.
[23] Du F, Ma Y, Lv X, Huang Y, Li F, Chen Y. The synthesis of single-walled carbon nanotubes with controlled length and bundle size using the electric arc method. Carbon 2006;44(7):1327–30.
[24] Schulz RB, Plantz VC, Brush DR. Shielding theory and practice. Electromagnetic Compatibility, IEEE Trans. 1988;30(3):187–201.
[25] Joo J, Epstein AJ. Electromagnetic radiation shielding by intrinsically conducting polymers. Appl. Phys. Lett. 1994;65(18):2278–80.
[26] Yussuf AA, Sbarski I, Hayes JP, Solomon M, Tran N. Microwave welding of polymeric-microfluidic devices. J. Micromech. Microeng. 2005;15(9):1692–9.
[27] Holzheimer T. A broadband materials measurements technique using the full frequency extent of the network analyzer. 2002 Anten. appl. symp. 2002.
[28] Kim B, Lee J, Yu I. Electrical properties of single-wall carbon nanotube and epoxy composites. J. Appl. Phys. 2003;94(10): 6724–8.
[29] Stauffer D, Aharony A. Introduction to Percolation Theory. Second ed. London: Taylor & Francis; 1992. 17-30.
[30] Park C, Ounaies Z, Watson KA, Crooks RE, Smith Jr J, et al. Dispersion of single wall carbon nanotubes by in situ polymerization under sonication. Chem. Phys. Lett. 2002;364(3):303–8.
[31] Grunlan JC, Mehrabi AR, Bannon MV, Bahr JL. Water-Based Single-Walled-Nanotube-Filled Polymer Composite with an Exceptionally Low Percolation Threshold. Adv. Mater. 2006;16(2): 150–153.
[32] Grimes CA, Mungle C, Kouzoudis D, Fang S, Eklund PC. The 500 MHz to 5.50 GHz complex permittivity spectra of single-wall carbon nanotube-loaded polymer composites. Chem. Phys. Lett. 2000;319(5-6):460–4.